

General Disclaimer

One or more of the Following Statements may affect this Document

- This document has been reproduced from the best copy furnished by the organizational source. It is being released in the interest of making available as much information as possible.
- This document may contain data, which exceeds the sheet parameters. It was furnished in this condition by the organizational source and is the best copy available.
- This document may contain tone-on-tone or color graphs, charts and/or pictures, which have been reproduced in black and white.
- This document is paginated as submitted by the original source.
- Portions of this document are not fully legible due to the historical nature of some of the material. However, it is the best reproduction available from the original submission.

NASA-CR-167736

(NASA-CR-167736) FLUID DYNAMIC AND
THERMODYNAMIC ANALYSIS OF A MODEL PERTAINING
TO CRYOGENIC FLUID MANAGEMENT IN LOW GRAVITY
ENVIRONMENTS FOR A SYSTEM WITH DYNAMICALLY
INDUCED SETTLING Final Report (Puerto Rico

M83-10091

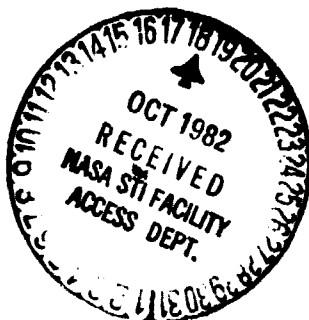
HC A05

Unclass

G3/12 35710

CONTRACT NAS9-16549

FLUID DYNAMIC AND THERMODYNAMIC ANALYSIS OF A MODEL
PERTAINING TO CRYOGENIC FLUID MANAGEMENT IN LOW
GRAVITY ENVIRONMENTS FOR A SYSTEM WITH
DYNAMICALLY INDUCED SETTLING

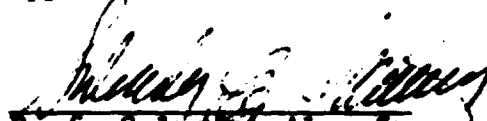



SCHOOL OF ENGINEERING
UNIVERSITY OF PUERTO RICO

Contract NAS9-16549

FLUID DYNAMIC AND THERMODYNAMIC ANALYSIS OF A MODEL
PERTAINING TO CRYOGENIC FLUID MANAGEMENT IN LOW
GRAVITY ENVIRONMENTS FOR A SYSTEM WITH
DYNAMICALLY INDUCED SETTLING

Approved:


Prof. Salvador Alemany
Chancellor


Dr. Fernando L. Benitez
Chairman
Mechanical-Nuclear
Engineering Department
School of Engineering

University of Puerto Rico
Mayaguez, Puerto Rico

**FLUID DYNAMIC AND THERMODYNAMIC ANALYSIS OF A MODEL
PERTAINING TO CRYOGENIC FLUID MANAGEMENT IN LOW
GRAVITY ENVIRONMENTS FOR A SYSTEM WITH
DYNAMICALLY INDUCED SETTLING**

By

Joe Ríos

July, 1982

Prepared Under

Contract NAS9-16549

Department of Mechanical and Nuclear Engineering

School of Engineering

Mayaguez Campus

University of Puerto Rico

Mayaguez, Puerto Rico

FOREWORD

This report presents the results of a study of some of the thermodynamic and fluid mechanics aspects pertaining to the management of cryogenic fluids in a system in which settling of the liquid and gaseous phases of the fluid is achieved through the use of a dynamic device (a helical screw) located within the propellant tank.

The study was performed under contract NAS9-16549.

ABSTRACT

The settling behavior of the liquid and gaseous phases of a fluid in a propellant tank in a zero-g environment, when such settling is induced through the use of a dynamic device, in this particular case, a helical screw was studied. Particular emphasis was given to: (1) the description of a fluid mechanics model which seems applicable to the system under consideration, (2) a First Law of Thermodynamics analysis of the system, and (3) a discussion of applicable scaling rules.

TABLE OF CONTENTS

	Page
Foreword	iii
Abstract	iv
Table of Contents	v
List of Figures	vi
Introduction	1
Technical Discussion	
A. General Considerations	4
B. Development of a Model	
Suitable for the Description	
of the Fluid Mechanics	
Behavior of the System	7
C. Thermodynamic Considerations	23
D. Power Requirements	47
E. Comments and Computational	
Procedure	56
F. Similarity Analysis and Model	
Testing	62
Conclusion	71
References	72

LIST OF FIGURES

		Page
Figure A-1	Helical screw-tank arrangement	4
Figure A-2	Helical screw	5
Figure B-3	Relationship between $V_{f/s}$, $V_{f/t}$ and $V_{s/t}$	9
Figure B-4	Velocity diagram for the case in which $V_{f/s} = 0$	10
Figure B-5	Velocity diagram for the case in which $\vec{V}_{f/t} = \vec{V}^1$	11
Figure B-6	Velocity diagram for the case in which $V > V^1$	12
Figure B-7	Velocity diagram for the case in which $1 > S > 0$	13
Figure B-8	Velocity diagrams for particles at r_1 , r_2 and r_3	14
Figure B-9	Velocity diagrams at $r = 0$ and $r = R_s$	15
Figure B-10	Distribution of the tangential velocity components of the fluid.	17

List of Figures (Cont.)	Page
Figure B-11 Velocity components for a particle of fluid in cylindrical coordinates (r, θ , z)	18
Figure B-12 Settling configuration . . .	21
Figure C-13 Control volume	23
Figure C-14 Fluid configuration for rotational kinetic energy considerations	39
Figure C-15 Differential element of mass	42
Figure D-16 Flow configuration between the tip of the screw and the tank wall	49
Figure D-17 Channel-like conduit through the helical screw	53
Figure D-18 Relation between P, α , and s.	54
Figure E-19 Inside of the screw shaft used as a return path for the liquid.	57

INTRODUCTION

The advent of space flight and the problems which have arisen in the management of cryogenic fluids in low or other adverse g conditions, in particular, those concerning withdrawal of the proper phase of a fluid, either the liquid or the gaseous one, from a propellant tank, have led to the proposal of several solutions to the problem.

Some of the proposed ideas have led to the development of hardware which has demonstrated the capabilities and feasibility, as well as the limitations of the concepts, especially in view of the application for which they were intended.

Engine restart, for example, requires some sort of device to retain and subsequently supply enough liquid to the engine's feed line during the initial moments when the engine is fired, until the main body of liquid is settled by the thrust force.

However, it is probably undesirable to rely on thrust forces to achieve settling of the phases for the purpose of transferring large quantities of cryogens between tanks in space, because of the time required by the transferring process.

Passive devices (those needing no external means to achieve the outflow of the required phase), especially of the screen type, will probably be the first choice for a transferring process. Certain devices of the dynamic type (those driven by an external energy source) which have been proposed, look as attractive alternatives for this purpose.

This study analyzes the behavior of a system in which the settling of the phases is achieved through the use of an externally driven device located inside the propellant tank, and establishes procedures for the determination of some of the more interesting parameters of the system. The device used is a helical screw. The tank is cylindrical with hemispherical ends, and the

axis of rotation of the screw lies along the longitudinal axis of the tank. The screw runs from one end of the tank to the other with a very little clearance between the tip of the screw blade and the tank's wall.

The external energy supplied to the screw is transferred to the fluid through body forces. Some of the energy is dissipated through frictional effects due to the viscosity of the fluid.

TECHNICAL DISCUSSION

A. GENERAL CONSIDERATIONS

The system studied, consists of a helical screw rotating within a cylindrical tank (Figure A-1). Power

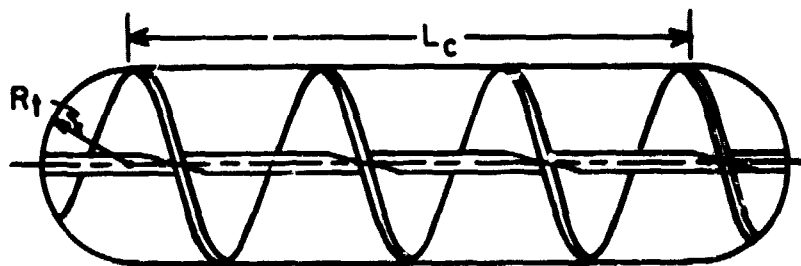


Fig. A-1. Helical screw-tank arrangement

to rotate the screw is supplied from an external source. The ends of the tank are hemispherical.

The length of the cylindrical portion of the tank is denoted by L_c , while the radius of the hemispherical ends is denoted by R_t . The latter is of the same length as the radius of the cylindrical section.

The following parameters characterize the helical screw (Figure A-2): diameter, helix angle, pitch, flight number, flight depth and screw length.

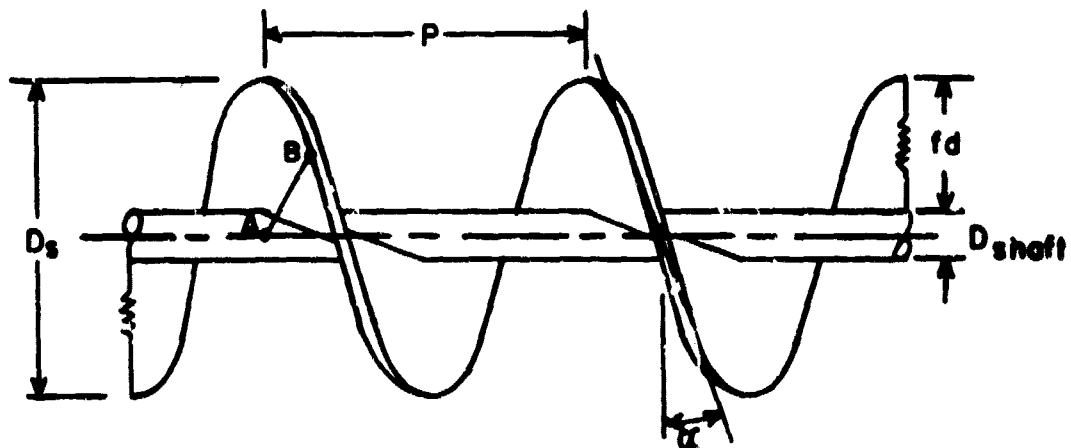


Fig. A-2. Helical screw

The screw diameter, D_s , is the diameter of an imaginary cylinder into which the screw would closely fit. The angle at which the helix cuts the normal circular section of this cylinder is the helix angle α . A flight

is one complete turn (360°) of the screw helix. The pitch, P , is the linear distance between adjacent flights. The screw length is determined by the longitudinal length of the tank since the helical screw should extend from one end of the tank to the other. The flight depth, fd , is the radial distance measured from the root to the tip of the helix. The helix is a right one which means that a line, such as A-B, drawn in a radial direction and lying on the surface of the screw, is perpendicular to the longitudinal axis of the screw. (Helical screws in which the line A-B makes an angle with respect to the axis different from 90° are also possible, but only a right one will be considered in the analysis which follows).

**B. DEVELOPMENT OF A MODEL SUITABLE FOR THE DESCRIPTION
OF THE FLUID MECHANICS BEHAVIOR OF THE SYSTEM.**

As the helical screw turns at the rate of N revolutions in unit time, a point in a fixed "nut" engaged to the screw would advance a distance equal to the pitch P in each revolution of the screw. Thus, the rate of advance V' of the point would be

$$V' = NP \quad (B1)$$

However, a fluid particle would advance in a direction parallel to the axis of rotation of the helical screw with a speed V which would depend upon the slip, defined as the excess of V' over V . Defining the ratio of the slip to V' as the slip ratio, S , then

$$S = \frac{V' - V}{V} = 1 - \frac{V}{V'} = 1 - \frac{V}{NP} \quad (B2)$$

Introducing the pitch to diameter ratio, λ ,
i. e.,

$$\lambda = \frac{P}{D_s} \quad (B3)$$

then,

$$S = 1 - \frac{V}{N\lambda D_s} \quad (B4)$$

Defining the advance ratio, J , as

$$J = \frac{V}{ND_s} \quad (B5)$$

then,

$$S = 1 - \frac{J}{\lambda} \quad (B6)$$

J , S , and λ are non-dimensional quantities and form part of the scaling laws of the system.

The velocity of a particle of the fluid can be described by either a frame of reference fixed with respect to the tank or by a frame of reference fixed with respect to the screw.

Let $V_{f/s}$ be the velocity of a particle of the fluid as seen by an observer located on the rotating screw. Since adjacent flights of the screw provide a channel through which the fluid can flow, the velocity of the fluid, $V_{f/s}$, would be directed essentially along lines parallel to the surface of the screw, as shown in Figure B-3.

Let $V_{f/t}$ be the velocity of the particle as seen by an observer fixed with respect to the tank, while $V_{s/t}$ is the velocity of a point in the helical screw as seen by the same observer. The latter velocity is always tangent to the circle traced by the point as the shaft rotates.

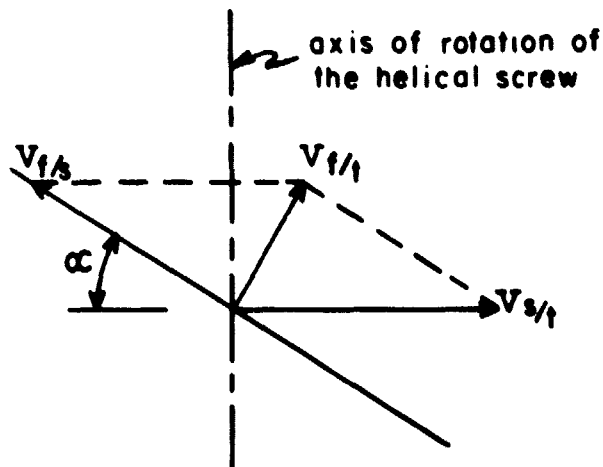


Fig. B-3. Relationship between $V_{f/s}$, $V_{f/t}$ and $V_{s/t}$

The relationship between $V_{f/s}$, $V_{f/t}$, and $V_{s/t}$ is shown in Figure B-3 and is given by

$$\vec{V}_{f/t} = \vec{V}_{s/t} + \vec{V}_{f/s} \quad (B7)$$

Several flow conditions will be examined as follows:

- a) Suppose $V_{f/s} = 0$. The corresponding velocity diagram is shown in Figure B-4. In this case, the particle does not advance in the direction of the axis of the screw, but performs a rigid body rotation with the screw. Thus $V = 0$ and $S = 1$.

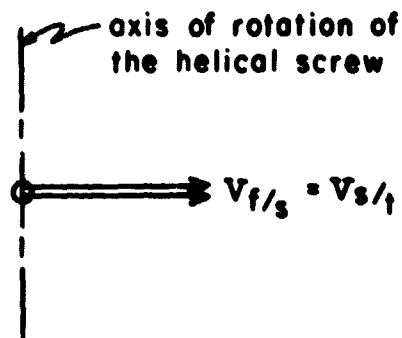


Fig. B-4. Velocity diagram for the case in which $V_{f/s} = 0$

- b) Consider the situation in which $\vec{V}_{f/t} = \vec{V}'$.

The corresponding velocity diagram is shown in Figure B-5. In this case $V = V'$ and $S = 0$. The particle's advance along a direction parallel to the axis of the screw corresponds to the advance that a point in a fixed 'nut' engaged in the screw would experience.

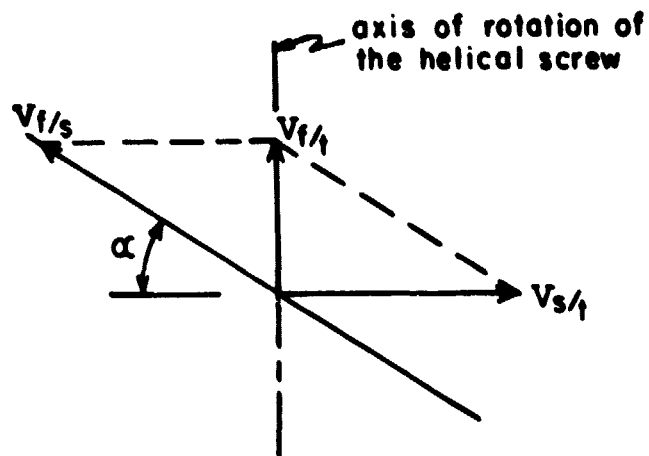


Fig. B-5. Velocity diagram for the case in which $\vec{V}_{f/t} = \vec{V}'$.

- c) Figure B-6 shows the velocity diagram for the case in which $V > V'$ so that $S < 0$.

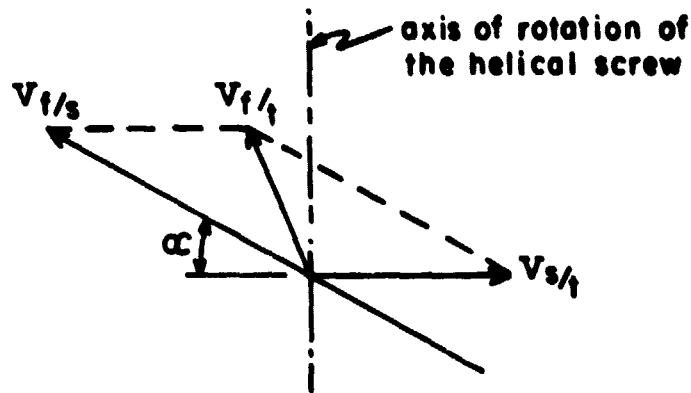


Fig. B-6. Velocity diagram for the case in which $V > V'$

The magnitude of $V_{f/t}$ and of $V_{f/s}$ are larger than those of the previous case for the same value of V .

- d) The velocity diagram, for the case in which $V_{f/t}$ and $V_{f/s}$ are smaller than those in (b) for the same value of V , is shown in Figure B-7. The value of S lies between 1 and 0, approaching the latter value as the particle approaches rigid body rotation about the axis of the screw.

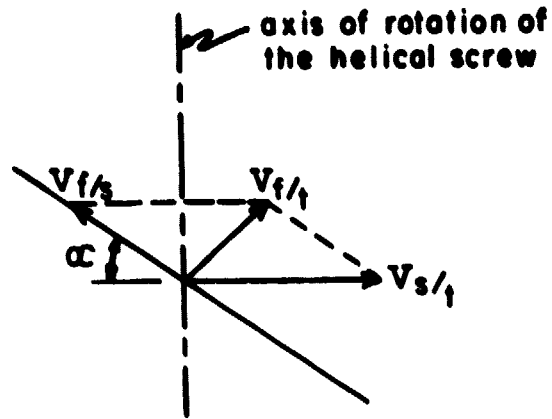


Fig. B-7. Velocity diagram for the case in which $1 > S > 0$

Thus far, the velocity diagrams for a single particle have been considered. We will now consider the velocity diagrams for a set of particles lying on a radial direction. Since the tangential velocity of points in the screw relative to the tank, $V_{s/t}$ varies linearly with radius, it is immediately apparent that we will have different velocity diagrams at different radii. Furthermore, these velocity diagrams will depend on the magnitude of the axial component of the velocity of the fluid with respect to the tank (i. e. V) for all points of a cross section normal to the longitudinal axis of the tank.

-14-

In our model, this component will be assumed to be of the same magnitude for all the points of the cross section.

Figure B-8 shows the resulting velocity diagrams for three particles located at radius r_1 , r_2 and r_3 .

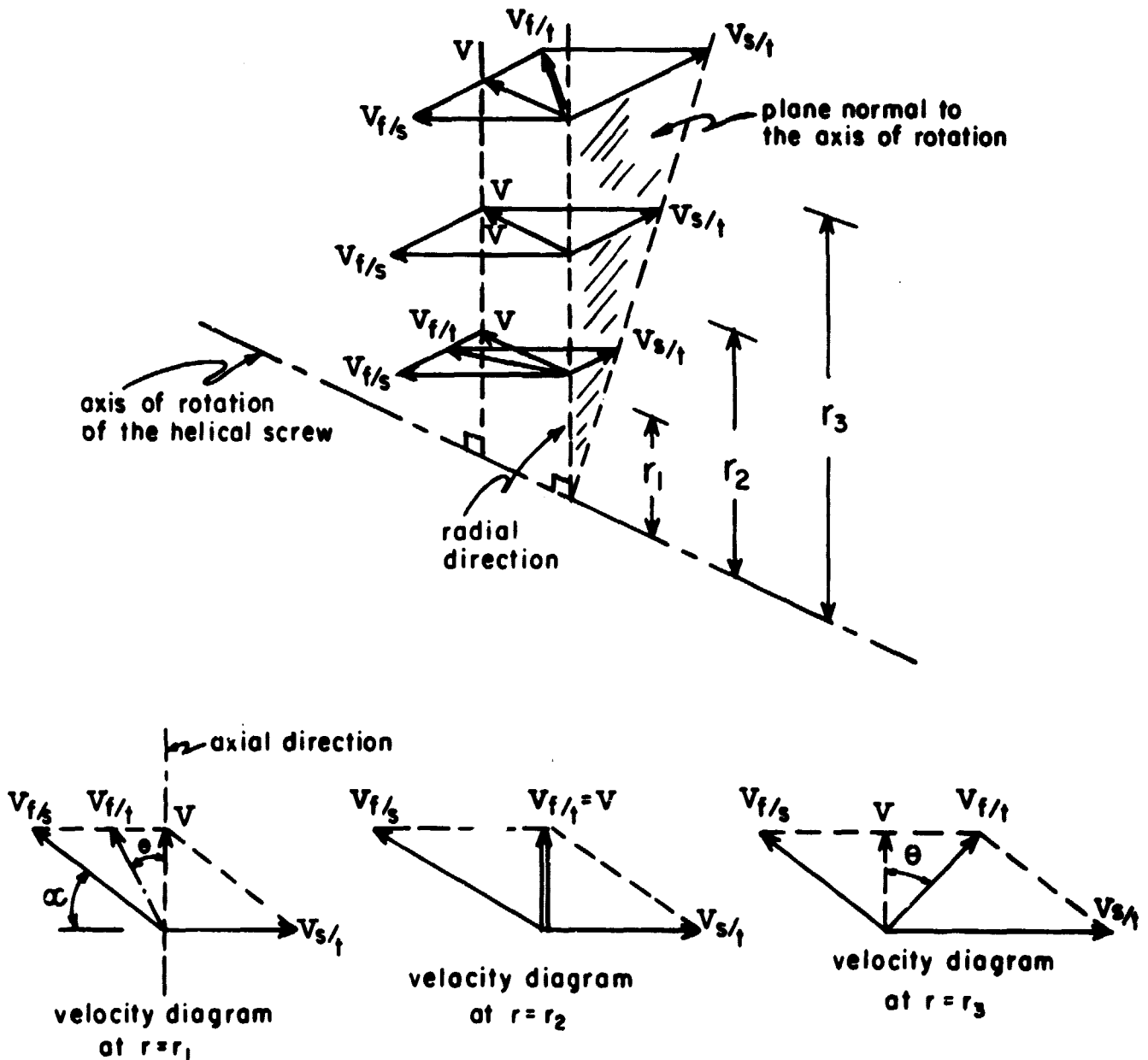


Fig. B-8. Velocity diagrams for particles at r_1 , r_2 and r_3

It is evident from these velocity diagrams that the fluid particles would move toward the fore end of the tank (the end toward which the screw seems to advance) following at different radii, different trajectories.

Figure B-9 shows the velocity diagram at a radius $r=0$ (at the root of the helical screw, if the diameter of the screw shaft is disregarded) and at $r=R_s$ (at the outer tip of the screw).

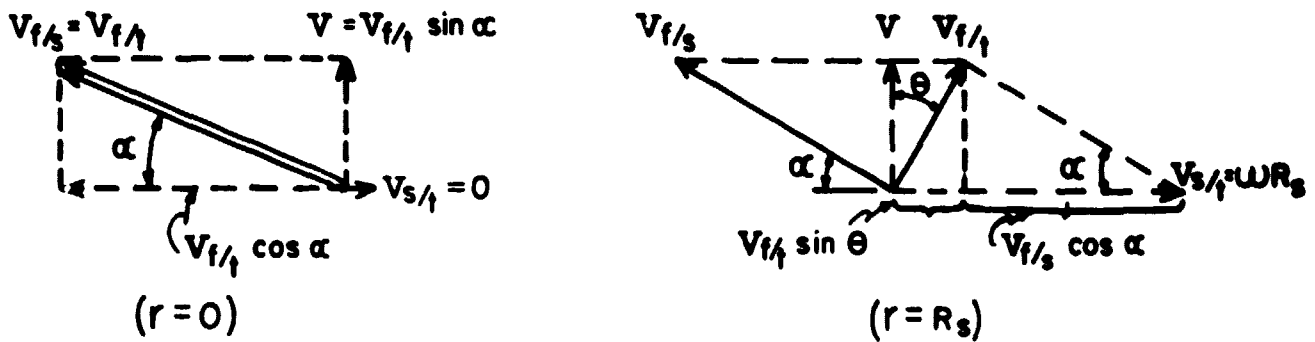


Fig. B-9. Velocity diagrams at $r = 0$ and $r = R_s$

The tangential component of the velocity of the fluid with respect to the tank is given by

$$V_{f/t} \cos \alpha = V \cot \alpha \quad (B8)$$

for $r = 0$, while at $r = R_s$ is given by

$$V_{f/t} \sin \theta = (V_{s/t}) R_s - V_{f/s} \cos \alpha \quad (B9)$$

$$= \omega R_s - V \cot \alpha \quad (B10)$$

(since $V_{f/s} \sin \alpha = V_{f/t} \cos \theta$), or at any radius by

$$\omega r - V \cot \alpha \quad (B11)$$

The distribution of these tangential velocity components, for the particles of fluid lying on a plane normal to the axis of rotation, is as shown in Figure B-10.

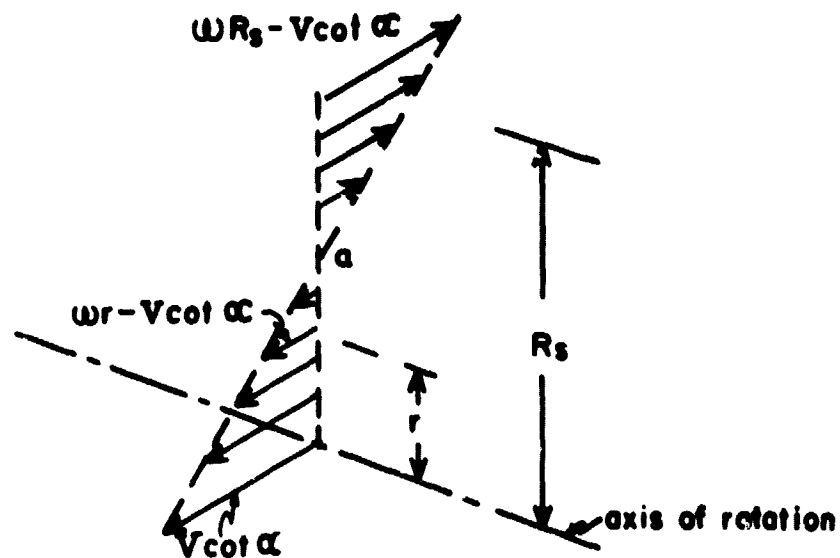


Fig. B-10. Distribution of the tangential velocity components of the fluid.

The velocity components for a particle of the fluid in cylindrical coordinates (r, θ, z) are shown in Figure B-11. The coordinate system is fixed with respect

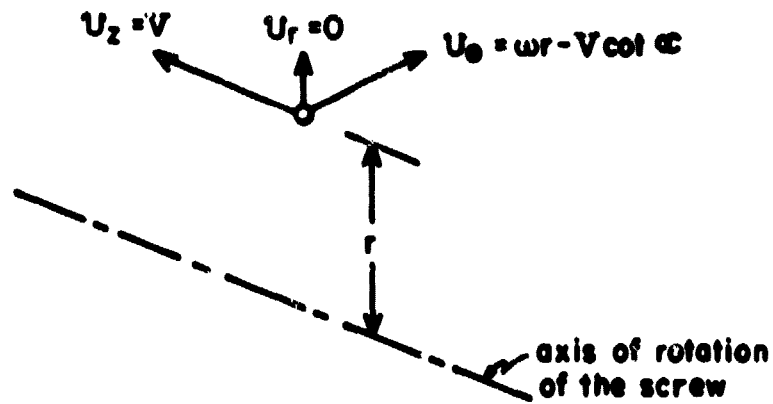


Fig. B-11. Velocity components for a particle of fluid in cylindrical coordinates (r, θ, z)

to the tank. The velocity field is thus described by

$$V_r = 0 \quad (B12)$$

$$V_\theta = \omega r - V \cot \alpha \quad (B13)$$

$$V_z = V \quad (B14)$$

Substitution of this velocity field into the Navier-Stokes equations, with the assumptions that the fluid is inviscid and subjected to a zero g condition, yields the relations.

$$\frac{\partial p}{\partial r} = \frac{\rho \cdot (\omega r - V \cot \alpha)^2}{r} \quad (B15)$$

$$\frac{\partial p}{\partial \theta} = 0 \quad (B16)$$

and $\frac{\partial p}{\partial z} = 0 \quad (B17)$

From (B17), the pressure field, p , can be described as

$$p = K + f_1(r, \theta)$$

where

$$K = \text{constant}$$

The mixed derivatives $\partial^2 p / (\partial r \partial \theta)$ and $\partial^2 p / \partial \theta \partial r$ are identical, so that the given velocity field is a solution to the equations.

Integrating the system of equations results in:

$$p = p_g + \frac{\rho \omega^2 (r^2 - R_g^2)}{2} - (2 \rho \omega V \cot \alpha) (r - R_g) + (\rho V^2 \cot^2 \alpha) \ln \frac{r}{R_g} \quad (B18)$$

where, p_g , is the pressure of the fluid at a radius R_g .

For a partially filled tank, since the pressure at the free surface of the liquid is uniform, the above equation indicates that the free surface of the liquid should be located at the same radial distance along the tank. Furthermore, since the equation indicates that the pressure increases with r , considering that the pressure of the gaseous phase is constant throughout the region it

-21-

occupies would limit the pressure distribution given by the above equation to the values of r for which $R_s \leq r \leq R_g$. R_s is the radius of the screw and R_g the radius at which the free surface is located. (Pressure variations within the gaseous phase would be negligible due to the order of magnitude of the density of the gaseous phase).

The above conclusions are illustrated in Figure B-12.

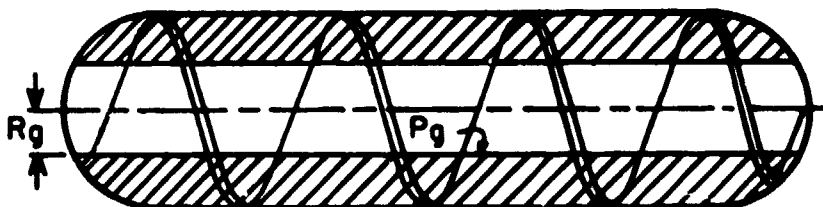


Fig. B-12. Settling configuration

If the mass of liquid is rotating as a rigid body, i. e. $V = 0$, then the pressure distribution is given by

$$p = p_g + \frac{\rho \omega^2 (r^2 - R_g^2)}{2} \quad (B19)$$

In this case also, the free surface of the liquid stands as shown in Figure B-12.

The above results points to an interesting design consideration in this model: the outlet for the liquid should be located at the periphery of the fore end of the tank.

-23-

C. THERMODYNAMIC CONSIDERATIONS

From a thermodynamic point of view, the model is described by the system shown in Figure C-13. The liquid and gaseous portions within the tank are enclosed by a control surface. Work, in the form of paddle-wheel work, as well as heat, cross the boundary of this surface. Liquid is withdrawn from the control surface at a constant rate while pressurant gas is added to maintain the pressure inside it constant. The pressurant gas is supplied at the temperature of the system. The latter is assumed constant during the process.

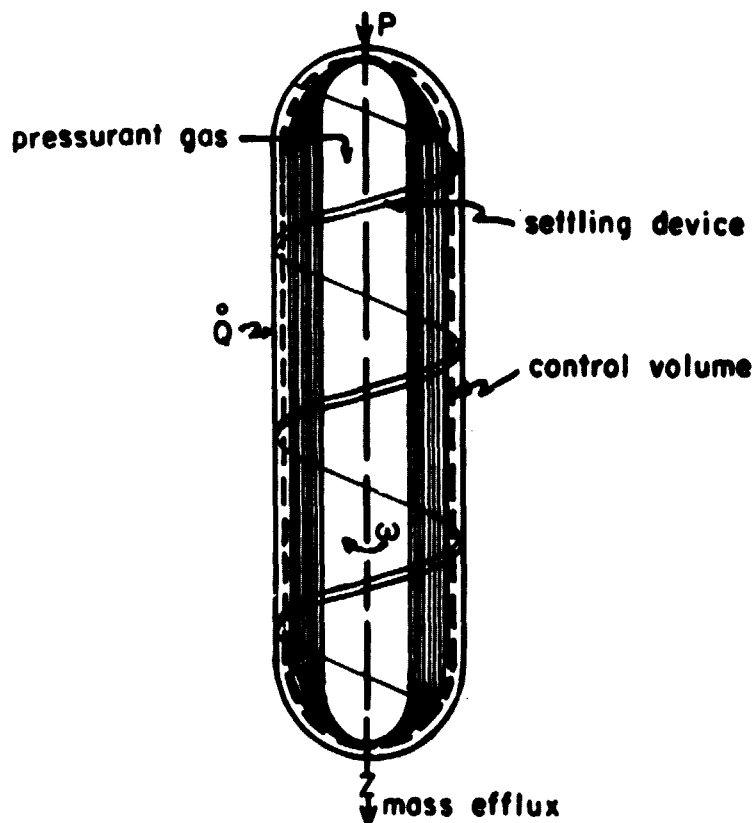


Fig. C-13. Control volume

Application of the First Law of Thermodynamics to the system results in:

$$\delta W + \delta Q - dm_e \left[\frac{V_e^2}{2g_c} + h_e \right] + dm_p \left[\frac{V_p^2}{2g_c} + h_p \right] = d(E\sigma) \quad (C1)$$

on as a rate equation as:

$$\frac{\delta W}{dt} + \frac{\delta Q}{dt} - \frac{dm_e}{dt} \left[\frac{V_e^2}{2g_c} + h_e \right] + \frac{dm_p}{dt} \left[\frac{V_p^2}{2g_c} + h_p \right] = \frac{d}{dt} (E\sigma) \quad (C2)$$

where,

$\frac{\delta W}{dt}$ = rate at which paddle-wheel work is supplied

$\frac{\delta Q}{dt}$ = rate at which heat is added to the system

$\frac{dm_e}{dt}$ = rate of mass efflux (liquid) from the tank

$\frac{dm_p}{dt}$ = rate of mass influx of pressurant gas into the tank

$\frac{v^2}{2g_c}$ = kinetic energy of the fluid entering or leaving the control volume

h = specific enthalpy of the mass of fluid leaving or entering the control volume.

$\frac{d}{dt}(E\sigma)$ = rate of change in energy content within the control surface.

(subscript σ refers to conditions within the control volume. Subscript p refers to the state of the pressurant gas as it enters the control volume and subscript e refers to the state of the liquid as it flows out of the control volume).

Changes in gravitational potential energy are assumed zero. Local properties are assumed constant during the process.

The energy content within the control volume comprises internal energy U , rotational kinetic energy E_r and translational kinetic energy E_k , i. e.,

$$E_{\sigma} = [U + E_r + E_k]_{\sigma} \quad (C3)$$

so that

$$\frac{d}{dt} (E_{\sigma}) = \frac{d}{dt} [U + E_r + E_k]_{\sigma} \quad (C4)$$

or

$$\frac{d}{dt} (E_{\sigma}) = \frac{d}{dt} [U]_{\sigma} + \frac{d}{dt} [E_r]_{\sigma} + \frac{d}{dt} [E_k]_{\sigma} \quad (C5)$$

The internal energy within the control volume consists of the sum of the internal energies of the liquid (U_l) and gaseous (U_g) phases in it, i. e.,

$$U = U_l + U_g \quad (C6)$$

The internal energy of the gaseous phase consists of the sum of the internal energies of the propellant vapor U_v and of the pressurant gas U_p .

Thus,

$$U = U_l + U_v + U_p \quad (C7)$$

$$= m_l \mu_l + m_v \mu_v + m_p \mu_p$$

where,

m_l , m_v , and m_p = the mass of the liquid, propellant vapor, and pressurant gas, respectively.

and,

μ_l , μ_v , and μ_p = the specific internal energies of the liquid, propellant vapor, and pressurant gas, respectively.

Differentiating (C7),

$$dU = d(m_1 \mu_1) + d(m_v \mu_v) + d(m_p \mu_p) \quad (C8)$$

If the gaseous mixture is assumed saturated with propellant vapor, then at a given instant of time, its composition can be determined as follows: its pressure, p , is due to the partial pressures of the propellant vapor and pressurant gas.

$$p = p_v + p_p \quad (C9)$$

also,

$$y (V_p) = (1-y) V_v \quad (C10)$$

and

$$\mu = y (\mu_p) + (1-y) \mu_v \quad (C11)$$

where,

p = total pressure of the gaseous mixture

p_v = partial pressure of the propellant vapor

p_p = partial pressure of the pressurant gas

V_v = specific volume of the propellant vapor

V_p = specific volume of the pressurant gas

μ = specific internal energy of the gaseous mixture

μ_v = specific internal energy of the propellant vapor

μ_p = specific internal energy of the pressurant gas

y = ratio of the mass of pressurant gas to the mass of the gaseous mixture, i. e.,

$$y = \frac{m_p}{m_p + m_v} \quad (C12)$$

From a table of properties for the propellant vapor, one obtains the following properties for the saturated vapor state, at the temperature, T , of the mixture:

$$P_v = (p \text{ sat.})_T \quad (C13)$$

$$V_v = (V_g)_T \quad (C14)$$

$$\mu_v = (\mu_g)_T \quad (C15)$$

The partial pressure of the pressurant gas is then

$$P_p = P - P_v \quad (C16)$$

Assuming that the pressurant gas behaves as an ideal gas,

$$v_p = \frac{R_p T}{P_p} \quad (C17)$$

Now,

$$\frac{y}{1-y} = \frac{V_v}{V_p} = \frac{(V_g)_T}{(R_p T/P_p)} \quad (C18)$$

Solving for y ,

$$y = \frac{1}{\left[1 + \frac{R_p T}{(V_g)_T P_p} \right]} \quad (C19)$$

y is the ratio of the mass of pressurant gas to the mass of the mixture, so that $(1-y)$ is the ratio of the mass of propellant vapor to the mass of the mixture.

The gas constant of the mixture can be expressed as

$$R = y R_p + (1-y) R_v \quad (C20)$$

where,

R_p = gas constant of the pressurant gas

R_v = gas constant of the propellant vapor

The mass of the gaseous mixture can be determined from

$$m = \frac{p V_g}{R T} \quad (C21)$$

where,

V_g = volume of the gaseous mixture.

The mass of propellant vapor is then

$$m_v = (1 - y) m \quad (C22)$$

and the mass of pressurant gas is

$$m_p = y m \quad (C23)$$

Consider now the equilibrium composition of the gaseous mixture at a later instant of time. Assume that the efflux of liquid has been such that the volume of the gaseous mixture has increased to V_{g2} . The composition of the gaseous mixture depends upon temperature and pressure. Since we are assuming them to be constant, the properties for the saturated vapor state at the temperature of the mixture remains constant. Following the procedure outlined previously, we will conclude that y , and thus R , do not vary during the process.

The mass of the gaseous mixture will depend upon the new volume of the mixture, V_{g2} , i. e.,

$$m_2 = \frac{P V_{g2}}{RT} \quad (C24)$$

The mass of propellant vapor is now,

$$m_{v2} = (1 - y) m_2 \quad (C25)$$

and that of the pressurant gas,

$$m_{p2} = y m_2 \quad (C26)$$

The change in the mass of propellant vapor in the mixture is

$$\begin{aligned} \Delta m_v &= m_{v2} - m_v \\ &= (1-y) m_2 - (1-y) m \\ &= (1-y) (m_2 - m) \\ \Delta m_v &= (1-y) \left[\frac{P}{RT} \right] \left[V_{g2} - V_g \right] \quad (C27) \end{aligned}$$

and that of the pressurant gas,

$$\begin{aligned}
 \Delta m_p &= m_{p2} - m_p \\
 &= y m_2 - y m \\
 &= y (m_2 - m) \\
 \Delta m_p &= y \left[\frac{p}{RT} \right] \left[V_{g2} - V_g \right] \quad (C28)
 \end{aligned}$$

Thus, the mass influx of pressurant gas, as well as the change in the mass of the propellant vapor, are proportional to the change in volume of the gaseous mixture.

The mass of liquid, m_l , that occupied the space $(V_{g2} - V_g)$ is given by,

$$\Delta m_l = \frac{(V_{g2} - V_g)}{v_l} \quad (C29)$$

where,

v_l = specific volume of the liquid (taken as that of saturated liquid at the temperature T of the system).

Of the quantity, m_1 , the amount Δm_v remains in the gaseous phase, so that the mass of liquid which efflux from the system is

$$\begin{aligned}
 m_{\text{efflux}} &= \Delta m_1 - \Delta m_v \\
 &= \frac{(V_{g2} - V_g)}{v_1} - (1-y) \left[\frac{p}{RT} \right] [V_{g2} - V_g] \\
 &= \frac{(V_{g2} - V_g)}{v_1} \left[1 - (1-y) v_1 \left(\frac{p}{RT} \right) \right] \quad (C30)
 \end{aligned}$$

Since

$$1-y = \frac{v_p y}{v_v} \quad (C31)$$

then,

$$m_{\text{efflux}} = \frac{(V_{g2} - V_g)}{v_1} \left[1 - \frac{v_p y v_1}{v_v} \left(\frac{p}{RT} \right) \right] \quad (C32)$$

Using the relations,

$$y = \frac{m_p}{m} \quad (C23)$$

$$\Delta m_1 = \frac{(V_{g2} - V_g)}{v_1} \quad (C29)$$

and $pV = m RT \quad (C33)$

relation (C-32), reduces to

$$m_{\text{efflux}} = \Delta m_1 \left[1 - \frac{v_1}{v_v} \right] \quad (C34)$$

Recalling that

$$\Delta m_p = y \left[\frac{p}{RT} \right] \left[V_{g2} - V_g \right] \quad (C28)$$

The above can be substituted in (C34) so that (C32) simplifies to

$$m_{\text{efflux}} = \Delta m_p \left(\frac{v_p}{v_1} \right) \left[1 - \frac{v_1}{v_v} \right] \quad (C35)$$

which shows that the influx of pressurant gas is proportional to the efflux of liquid.

Consider now the change in internal energy within the control volume: U_{σ} can be expressed as,

$$\begin{aligned} U_{\sigma} &= m_1 \mu_1 + m_v \mu_v + m_p \mu_p \\ &= m_1 \mu_1 + \left[m_v \mu_v + m_p \mu_p \right] \end{aligned} \quad (C36)$$

Multiplying and dividing the terms within the brackets by $(m_v + m_p)$,

$$\begin{aligned} U_{\sigma} &= m_1 \mu_1 + (m_v + m_p) \left[\left(\frac{m_v}{m_v + m_p} \right) \mu_v + \left(\frac{m_p}{m_v + m_p} \right) \mu_p \right] \\ U_{\sigma} &= m_1 \mu_1 + (m_v + m_p) \left[(1-y) \mu_v + y \mu_p \right] \end{aligned} \quad (C37)$$

The term in the bracket now is μ , the specific internal energy of the gaseous mixture, which is constant.

Therefore,

$$U_{\sigma} = m_1 \mu_1 + (m_v + m_p) \mu \quad (C38)$$

Since μ_1 depends upon temperature and thus, is constant in our case, a change in the internal energy within the control surface is,

$$\begin{aligned}
 \Delta U_{\sigma} &= \mu_1 \Delta m_1 + \mu \Delta (m_v + m_p) \\
 &= \mu_1 \Delta m_1 + \mu \left[\Delta m_v + \Delta m_p \right] \\
 &= \mu_1 \Delta m_1 + \mu \left[\Delta m_1 \left(\frac{v_1}{v_v} \right) + \Delta m_1 \left(\frac{v_1}{v_p} \right) \right] \\
 \Delta U_{\sigma} &= \Delta m_1 \left[\mu_1 + \mu \left(\frac{v_1}{v_v} \right) + \mu \left(\frac{v_1}{v_p} \right) \right] \quad (C39)
 \end{aligned}$$

Substituting Δm_1 in terms of m_{efflux} ,

$$\Delta U_{\sigma} = \left[\mu_1 + \mu \left(\frac{v_1}{v_v} \right) + \mu \left(\frac{v_1}{v_p} \right) \right] \left[\frac{v_v}{v_v - v_1} \right] m_{\text{efflux}} \quad (C40)$$

The terms within the brackets are constant, so that ΔU_{σ} can be expressed as

$$\Delta U_{\sigma} = C_1 m_{\text{efflux}} \quad (C41)$$

where,

$$C_1 = \left[\mu_1 + \mu v_1 \left(\frac{v_v + v_p}{v_v v_p} \right) \right] \left[\frac{v_v}{v_v - v_1} \right] \quad (C42)$$

Consider now the change in rotational kinetic energy within the control volume. The instantaneous rotational kinetic energy is determined by summing the rotational kinetic energies for all the particles i within the control surface, i. e.,

$$E_r = \sum \frac{m_i w_{fi}^2 r_i^2}{2 g_c} \quad (C43)$$

For the fluid configuration shown in Figure C14 one can determine the rotational kinetic energy of

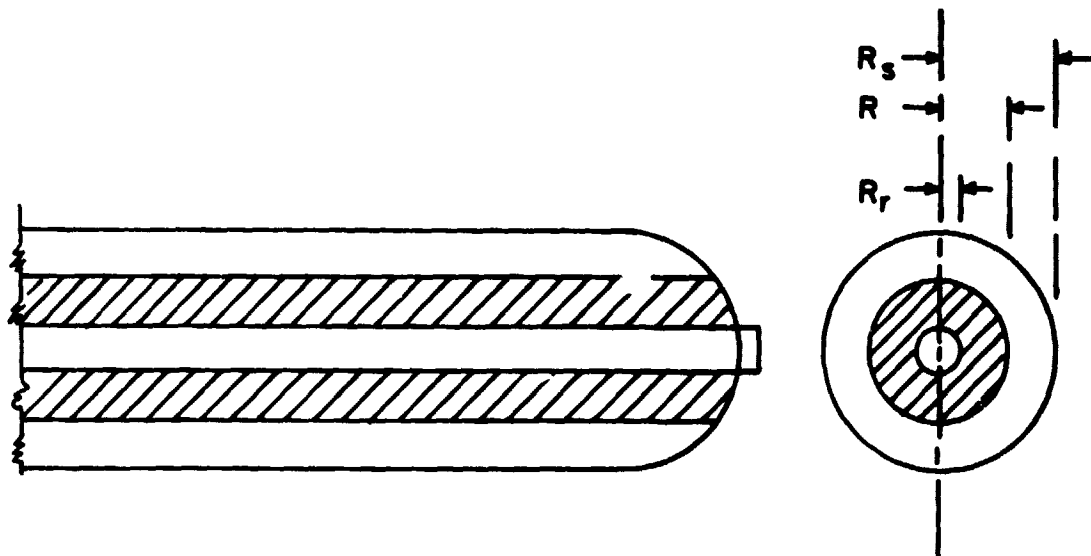


Fig. C-14. Fluid configuration for rotational kinetic energy considerations.

the particles for the section of the tank within radii, R_r and R , by the relation

$$E_r = \int_{R_r}^R \frac{r^2 \omega_f^2 dm}{2g_c} \quad (C44)$$

$(R_r \rightarrow R)$

where,

R_r = radius of the screw shaft

ω_f = angular velocity of the fluid particle

If the contribution of the gaseous phase to the rotational kinetic energy is neglected and the liquid is assumed to remain during the process in the configuration shown in Figure B-12, then (C44) would represent the rotational kinetic energy lost due to the efflux of mass, considering that the tank was initially full.

The mass within the differential element of volume in Figure C-15, is given by

$$dm = \rho (2\pi r dr) (L + 2 \ell) \quad (C45)$$

where,

L = length of the cylindrical portion of the tank

ℓ = variable length of the section at the hemispherical ends.

The relationship between ℓ , R_s and r is given by

$$\ell = \sqrt{R_s^2 - r^2} \quad (C46)$$

as shown in Figure C-15.

ORIGINAL PAGE IS
OF POOR QUALITY

-42-

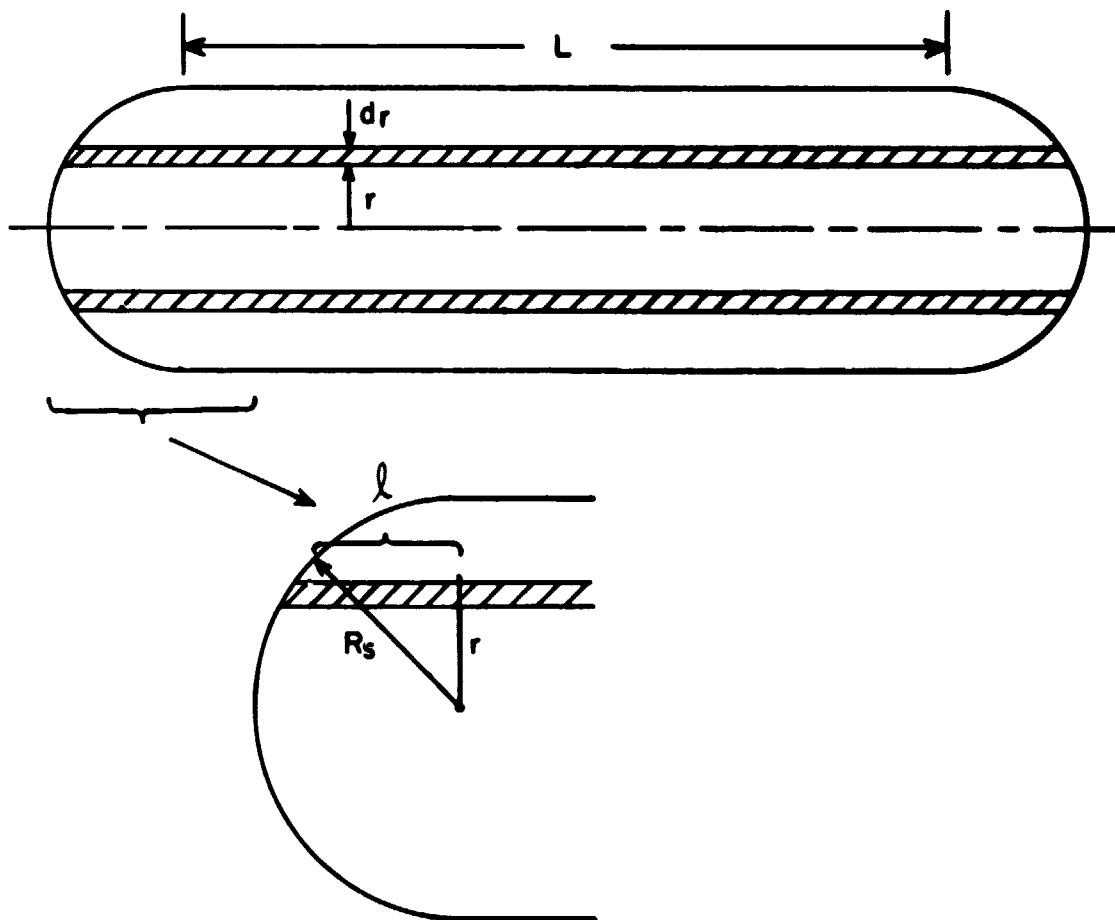


Fig. C-15. Differential element of mass

-43-

Thus,

$$dm = 2 \pi \rho \left[L + 2 \sqrt{R_s^2 - r^2} \right] r dr \quad (C47)$$

Dividing both sides by dt,

$$\frac{dm}{dt} = \left[2 \pi \rho L r + 4 \pi \rho r \sqrt{R_s^2 - r^2} \right] \frac{dr}{dt} \quad (C48)$$

gives the rate of change of the radius with respect to the rate of change of mass. It represents the rate of mass efflux of the liquid, \dot{m}_{efflux} , so that

$$\dot{m}_{\text{efflux}} = \left[2 \pi \rho L r + 4 \pi \rho r \sqrt{R_s^2 - r^2} \right] \frac{dr}{dt} \quad (C49)$$

Separating variables,

$$\dot{m}_{\text{efflux}} = \left[2 \pi \rho L r + 4 \pi \rho r \sqrt{R_s^2 - r^2} \right] dr$$

Integrating, considering \dot{m}_{efflux} constant, results in

$$t = \frac{\pi \rho}{\dot{m}_{\text{efflux}}} = \left[L (R^2 - R_r^2) + \frac{4}{3} \left(\sqrt{R_s^2 - R_r^2} \sqrt{R_s^2 - R^2} \right) \right] \quad (C50)$$

which is the time it takes to reach a radius R, starting at a radius R_r .

Neglecting R_r ,

$$t = \frac{\pi \rho}{\dot{m}_{\text{efflux}}} \left[L (R^2) + \frac{4}{3} \left(R_s^3 - (R_s^2 - R^2)^{3/2} \right) \right] \quad (\text{C51})$$

From (C44), the instantaneous rate of change of rotational kinetic energy is

$$\begin{aligned} \frac{dE_r}{dt} &= r^2 \omega_f^2 \frac{dm}{dt} \\ &= r^2 \omega_f^2 \dot{m}_{\text{efflux}} \end{aligned} \quad (\text{C52})$$

Substituting ω_f from (B11), results in

$$\frac{dE_r}{dt} = r^2 \left(\omega - \frac{V \cot \alpha}{r} \right)^2 \dot{m}_{\text{efflux}} \quad (\text{C53})$$

which is the quantity desired for the energy equation for the model under consideration.

Regarding the rate of translational kinetic energy lost due to the efflux of mass, it can be determined from

$$\frac{dE_k}{dt} = \frac{V^2}{2g_c} \frac{dm}{dt} = \frac{V^2}{2g_c} \dot{m}_{\text{efflux}} \quad (\text{C54})$$

-45-

So far we have examined the terms on the right hand side of the equation in (C2). On the left hand side of it, we have that

$$\frac{dm_e}{dt} = \dot{m}_{\text{efflux}} \quad (\text{C55})$$

and is related to V_e through

$$\dot{m}_{\text{efflux}} = A_e V_e \rho_l \quad (\text{C56})$$

where

A_e = cross sectional area of the exit pipe

ρ_l = density of the liquid leaving the tank.

The term \dot{m}_p is related to \dot{m}_{efflux} through equation (C35), and is related to V_p through

$$\dot{m}_p = A_p V_p \rho_p \quad (\text{C57})$$

where,

A_p = cross sectional area of the pressurant
gas inlet pipe

ρ_p = density of the pressurant gas

Substitution of the various relations derived into the energy equation (C2) would give the instantaneous relationship between power and heat transfer rate.

D. POWER REQUIREMENTS

The assumption of an inviscid liquid in Section B was reasonable for the purpose of obtaining values for the velocities of the bulk of the liquid. On the other hand, a large fraction of the power requirements are associated with viscous losses, and thus difficult to assess.

Discussion of a method for predicting power requirements for the model follows: If one considers that the tank is initially full and no efflux of liquid occurs, while the latter is brought from rest to the desired rotational speed, then the liquid would rotate approximately as a rigid body and the energy requirements for the liquid (disregarding that required by the helical screw itself) would correspond to the rotational kinetic energy of the liquid. It can be evaluated by integrating (C44) with $R = R_s$. Thus,

$$E_r = \pi \rho \left[\frac{\omega^2 L R_s^4}{4} + \frac{4}{15} \omega^2 R_s^5 \right] \quad (D-1)$$

If the time required to achieve the desired rotational speed for the helical screw is t , then the average power requirement during this initial period would be

$$P = \frac{E_r}{t} \quad (D-2)$$

Evidently, frictional and drag losses at the tip of the helical screw as well as inefficiencies of the driving device will contribute additional power requirements. These can be better handled through tests and related through an initial settling efficiency as:

$$e_s = \frac{\text{ideal power requirement}}{\text{actual power requirement}} \quad (D-3)$$

Once the screw has achieved the desired rotational speed, and the body of liquid rotates nearly as a rigid body, the fluid losses will be mainly due to viscous forces between the rotating body of liquid and the tank wall through the layer of liquid in the clearance space.

An estimate of this loss can be obtained as follows:
a cross-sectional view of the flow pattern at the tip of
the screw is shown in Figure D-16. The velocity of the
fluid at the tip of the screw is given by

$$U_{\infty} = \omega R_s = 2\pi N R_s \quad (D-4)$$

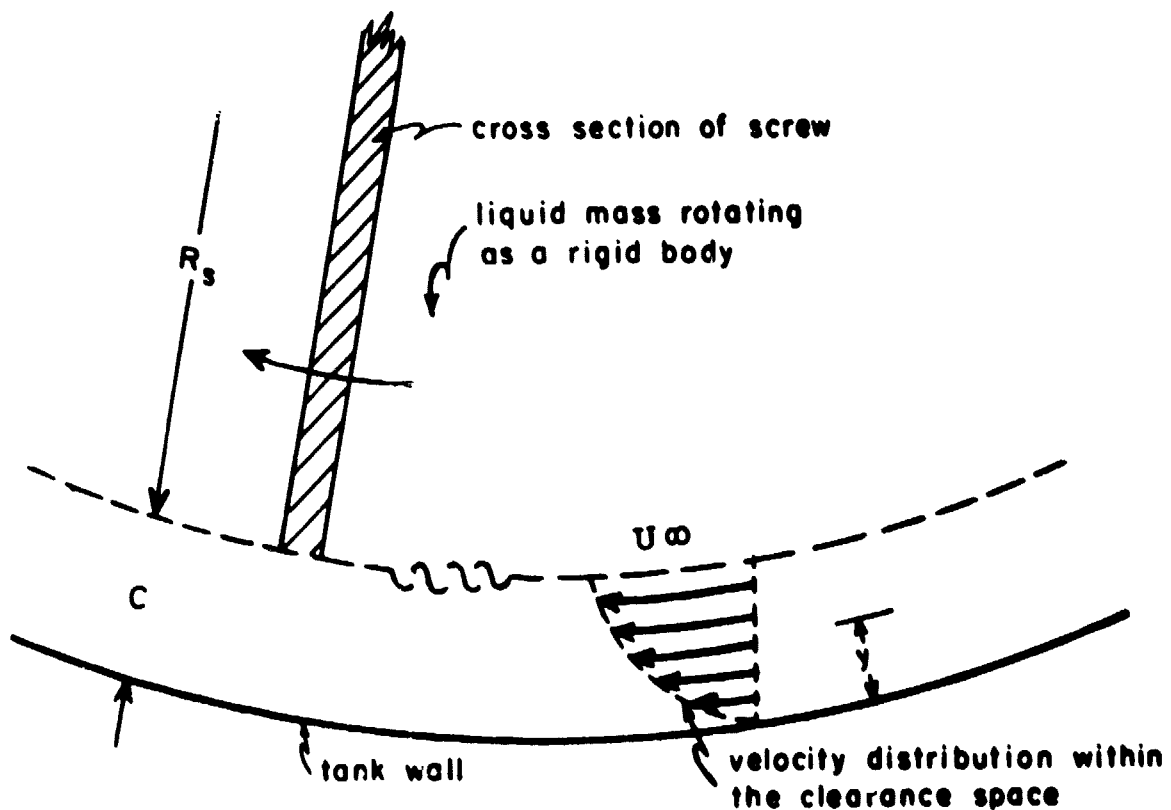


Fig. D-16. Flow configuration between the tip
of the screw and the tank wall.

while that of the fluid at the tank wall is assumed zero. Due to viscous effects a velocity distribution within the clearance space will be set up causing a shear stress and a corresponding drag force at the wall. The drag force can be estimated by applying the relations for flat plate boundary layers.

The drag force D is given by

$$D = b \int_0^x \tau_w(x) dx \quad (D5)$$

where,

b = length of the layer in the radial direction

x = length of the plate, in this case equal to the circumference of the tank

The shear stress at the wall, and correspondingly, the method of analysis for D , will depend upon flow conditions. If, for example, laminar flow is assumed in the clearance space, the shear stress at the wall will be given by

$$\tau_w = \mu \left. \frac{\partial u}{\partial y} \right|_{y=0} \quad (D6)$$

where,

y = perpendicular distance measured from
the wall

μ = viscosity of the liquid

Assuming a velocity distribution in the clearance
space as,

$$U = U_{\infty} \left(\frac{2y}{c} - \frac{y^2}{c^2} \right) \quad (D7)$$

then,

$$\tau_w = \frac{2\mu U_{\infty}}{c} \quad (D8)$$

The drag force is then,

$$D = \frac{2\mu U_{\infty}}{c} \left[2 \pi R_t b \right] \quad (D9)$$

where,

R_t = radius of the tank

Since the distance travelled per unit time by the tip of the screw is $2\pi R_s N$, the power required to overcome this frictional effect is

$$p = \frac{4 \pi \mu U^\infty R_t b}{c} \times 2\pi R_s N \quad (D10)$$

$$p = \frac{8\pi^2 R_t^2 R_s \mu U^\infty b N}{c} \quad (D11)$$

Substituting for U^∞ , results in,

$$p = \frac{16\pi R_t R_s^2 N^2 \mu b}{c} \quad (D12)$$

Care should be used in applying this relation to the hemispherical ends. In this case a mean radius and the proper value of b should be used.

In a similar way, frictional losses of this type can be determined in the case of turbulent flows.

Now then, when the valve at the discharge end of the tank opens, allowing an efflux of liquid, a velocity V_f/s

ORIGINAL PAGE IS
OF POOR QUALITY

-53-

of the fluid relative to the screw surface will develop. This velocity is related to V and the helix angle of the screw α by

$$V = V_f/s \sin \alpha \quad (D13)$$

To determine the frictional losses in this case, one can assume the liquid to be moving along a helical channel of rectangular cross section formed by the walls of the helix, the tank wall and the screw shaft as shown in Figure D-17.

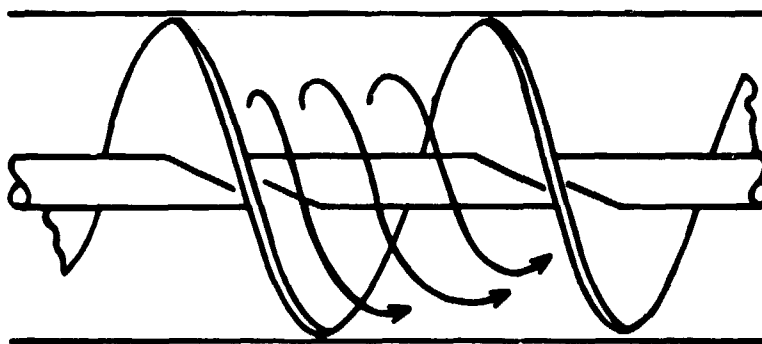


Fig. D17. Channel-like conduit through the helical screw.

ORIGINAL PAGE IS
OF POOR QUALITY

-54-

The standard procedure used for the determination of losses in noncircular pipes can, thus, be applied.

The cross sectional area, A_c , available for the flow is

$$A_c = R_t s$$

where,

$$s = P \cos \alpha$$

as shown in Figure D-18.

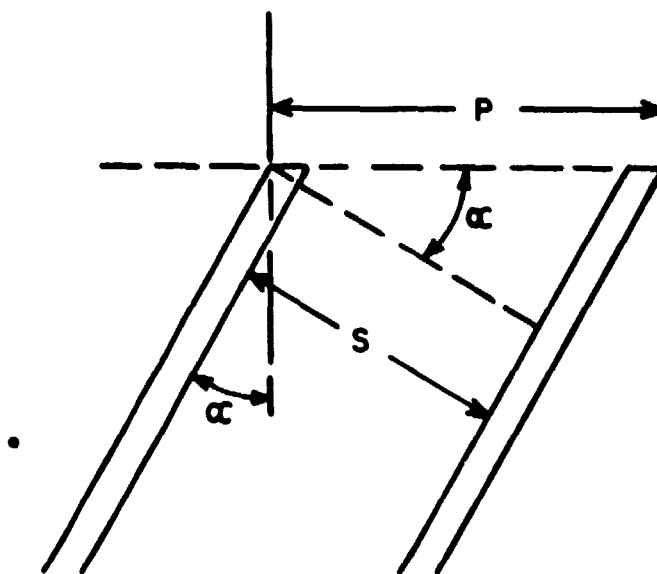


Fig. D-18. Relation between P , α , and s

The hydraulic diameter is given by

$$\begin{aligned} D_h &= \frac{4 \times \text{area}}{\text{wetted perimeter}} \\ &= \frac{4R_t s}{2 (R_t - R) + s} \end{aligned} \quad (D14)$$

Frictional losses in this case are determined by the use of the Moody Chart and standard procedures.

E. COMMENTS AND COMPUTATIONAL PROCEDURE

It is expected that a simple model as the one previously discussed has shortcomings. In this particular case, the shortcomings occur at both ends of the tank where boundary conditions are not satisfied by the velocity field chosen. This makes application of the model unsuitable for tanks with a small length to diameter ratio. It would be only applicable to large tanks, which probably comprise most of the storage vessels of practical use.

At the fore end of the tank, one would expect that, although the fluid has been moving toward that end with a uniform velocity, V , not all of the liquid finds its way out of the tank. The portion of liquid remaining in the tank would recirculate locally or would try to find its way towards the aft end. This would result in large viscous losses. An approach that could reduce viscous losses in the model, with the added advantage that flow conditions would be closer to those assumed, would be to provide a return path for the liquid through the helical screw shaft as shown in Figure E-19. The return path

ORIGINAL PAGE IS
OF POOR QUALITY

-57-

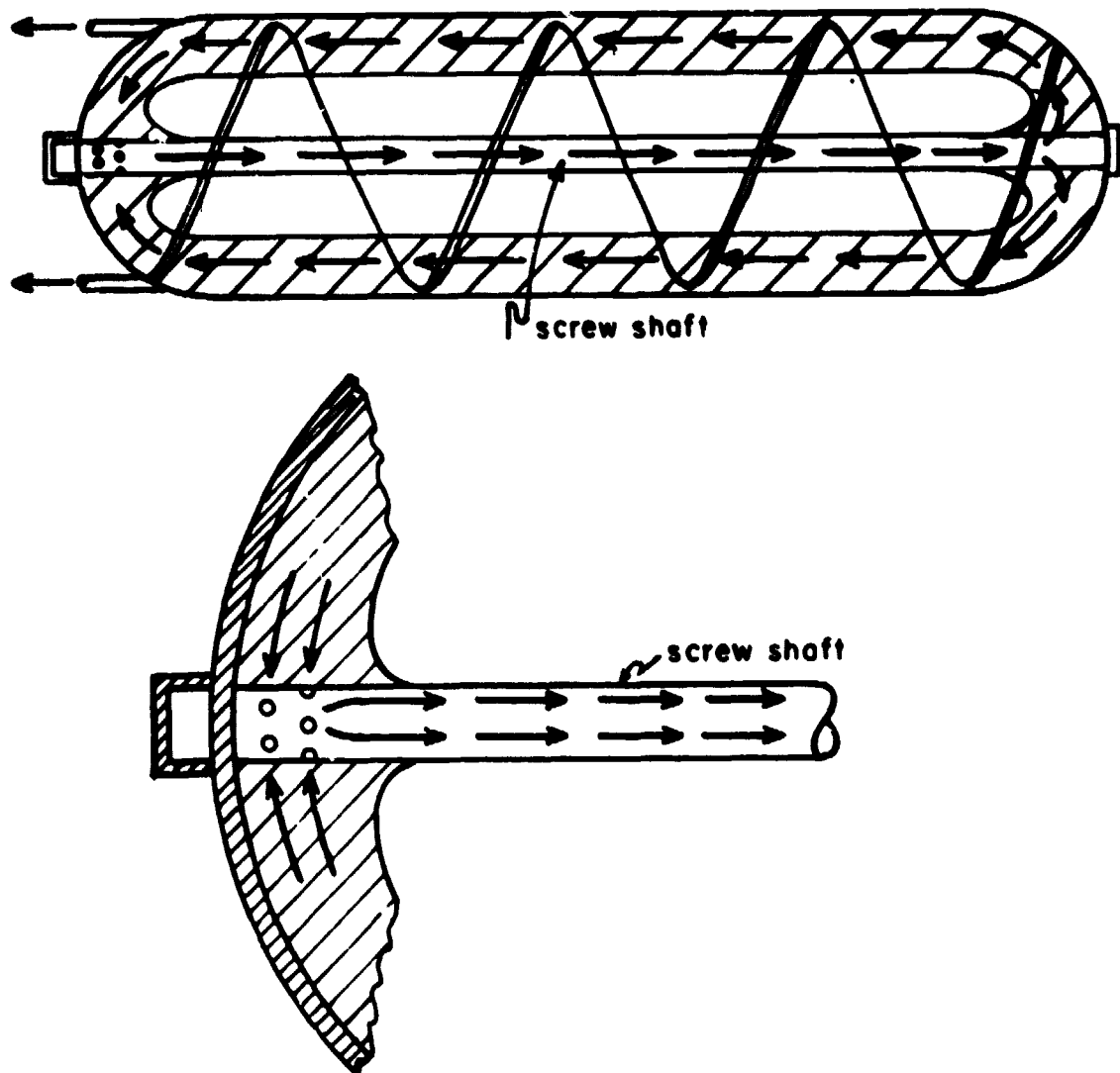


Fig. E-19. Inside of the screw shaft used as
a return path for the liquid

would also provide an escape route for any gas trapped at the fore end during the initial settling of the fluid.

The mass of liquid moving toward the fore end can be determined from

$$\dot{m} = A_w V \rho \quad (E1)$$

where,

$$A_w = \pi (R_s^2 - R^2) V \rho \quad (E2)$$

is the wetted portion of the screw's cross sectional area.

The rate of mass efflux \dot{m}_{efflux} would be a fraction K of \dot{m} , i.e.,

$$\dot{m}_{\text{efflux}} = K \dot{m} \quad (E3)$$

(1-K) would represent the fraction of \dot{m} which is recirculated.

Thus,

$$\dot{m}_{\text{efflux}} = K \pi \rho (R_s^2 - R^2) V \quad (E4)$$

A summary of the computational procedure is presented in what follows:

- a) the desired rotational speed is determined by the criteria set forth in Reference (3); the minimum rotational speed being given by

$$\omega = \sqrt{\frac{4\sigma g_c}{\rho_1 R_t^3}} \quad (E5)$$

- b) the helical screw is started and brought to the desired rotational speed. (A closed, full tank is assumed during this part of the process).
- c) the discharge valve is opened and the desired liquid efflux is established.
- d) pressurant flow rate is determined from (C35).
- e) a small time interval is selected so that conditions can be considered quasi-steady during it.
- f) the radius R reached at the end of the time interval is determined by either (C50) or (C51).

- g) the value of V is determined from (24) for an assumed value of K .
- h) the pressure distribution is determined using (B19).
- i) the change in internal energy within the control volume is determined from (C41).
- j) the change in the rotational kinetic energy and the translational kinetic energy is determined using (C53) and (C54) respectively.
- k) frictional losses are determined by the procedures of section D.
- l) V_e and V_p are evaluated from (C56) and (C57) respectively.
- m) thermodynamic properties of the fluid are obtained from appropriate tables.
- n) all terms are substituted in the energy equation and the instantaneous rate of heat transfer is determined.

- o) the value of R for the next interval of time is determined from (C50) or (C51).
- p) the process is repeated for each interval of time during the transfer process.

F. SIMILARITY ANALYSIS AND MODEL TESTING

Three types of similarity must be considered in settling systems. These are: geometric, kinematic and dynamic similarity.

Two systems are considered geometrically similar when the ratios of corresponding dimensions in one system to those of another have the same value. This implies that the systems, although of different sizes, have the same shape.

Kinematic similarity exists between two systems when, in addition to possessing geometric similarity, the ratios of velocities between corresponding points in each system have the same value.

Dynamic similarity exists between two systems when, in addition to being geometrically and kinematically similar, the ratio of forces between corresponding points have the same value.

The dimensionless groups pertinent to the settling system being considered are:

$$N_{Re} = \frac{\rho N D_s^2}{\mu} \quad (F1)$$

$$N_{we} = \frac{\rho N^2 D_s^3}{\sigma} \quad (F2)$$

$$N_{Fr} = \frac{D_s N^2}{g} \quad (F3)$$

$$J = \frac{V}{N D_s} \quad (F4)$$

$$N_{p1} = \frac{P^1}{\rho N^3 D_s^5} \quad (F5)$$

as well as the geometric ratios $\lambda = P/D_s$, D_s/D_t , D_s/c , D_s/L_t , D_s/D_r , D_s/D_e , and D_s/D_p ,

where,

N_{Re} = Reynolds number

N_{we} = Weber number

N_{Fr} = Froude number

J = advance ratio

- N_p = power number
- N = rotational speed of the helical screw
- D_s = diameter of the helical screw
- D_t = diameter of the tank
- c = clearance between the tip of the screw
and the tank wall
- ρ = density of the liquid
- μ = viscosity of the liquid
- P^1 = power supplied to the system
- P = pitch of the helical screw
- L_t = length of the tank
- σ = surface tension of the liquid
- D_r = diameter of the helical screw shaft
- D_e = diameter of the liquid discharge line
- D_p = diameter of the pressurant line
- g = gravitational acceleration
- V = axial velocity of the fluid (a function
of \dot{m}_{efflux})

The Weber and Froude number can be combined to form the Bond number, i.e.,

$$Bo = \frac{N_{we}}{N_{Fr}} = \frac{\rho D_s^2 g}{\sigma} \quad (F6)$$

Equality of all the groups assures similarity between systems of different size. The last seven dimensionless groups of the above list represent the groups necessary for geometric similarity which requires that all corresponding dimensions between a model and its prototype bear the same ratio to each other. The reference dimension used for the above group is the helical screw diameter.

Confining attention to geometrically similar systems would require equality of the following groups to insure dynamic and kinematic similarity:

$$N_{Re}, N_{we}, N_{Bo}, N_{p1}, J$$

An experimentally derived function correlating the data for such a system would be of the form

$$f\left(\frac{\rho N D_s^2}{\mu}, \frac{\rho N^2 D_s^3}{\sigma}, \frac{\rho D_s^2 g}{\sigma}, \frac{P^1}{\rho N^3 D_s^5}, \frac{V}{N D_s}\right) = 0 \quad (F7)$$

Consider the subscript m to represent the value of a property for a model while subscript p represents the value of the same property for its prototype.

Model testing requires that the values of corresponding dimensionless groups between model and prototype be the same. Test conditions that must be satisfied to insure similarity of solutions will be analyzed in what follows. To begin, consider the Froude number. To satisfy similarity conditions requires that the ratio of the Froude number of the prototype to the Froude number of the model satisfy

$$\frac{(N_{Fr})_p}{(N_{Fr})_m} = 1 \quad (F8)$$

$$\text{or} \quad \left(\frac{D_{sp}}{D_{sm}} \right)^2 \left(\frac{N_p}{N_m} \right) \left(\frac{g_m}{g_p} \right) = 1 \quad (F9)$$

Solving for N_m/N_p yields

$$\frac{N_m}{N_p} = \left(\frac{D_{sp}}{D_{sm}} \right)^2 \left(\frac{g_m}{g_p} \right) \quad (F10)$$

Considering g_m/g_p as 10^6 and D_{sp}/D_{sm} as 30, then

$$\frac{N_m}{N_p} = (30)^2 (10^6) = 9 \times 10^8 \quad (F11)$$

If the prototype were to turn at 6 rpm, the above relation means that testing at one g would require a rotational speed of

$$N_m = 5.4 \times 10^9 \text{ rpm} \quad (\text{F12})$$

which is an excessively high value.

However, if one assumes that the maximum rotational speed of the screw is 84 rpm, then, the maximum g level at which testing would be satisfactory would be,

$$\begin{aligned} \frac{g_m}{g_p} &= \left(\frac{N_m}{N_p} \right) \left(\frac{D_{sm}}{D_{sp}} \right)^2 \\ &= \left(\frac{84}{6} \right) \left(\frac{1}{30} \right)^2 \\ &= 1.6 \times 10^{-2} \end{aligned} \quad (\text{F13})$$

Preservation of similarity also requires that the ratio of Reynolds number also be 1. Thus,

$$\frac{(N_{Re})_p}{(N_{Re})_m} = \left(\frac{\rho_p}{\rho_m} \right) \left(\frac{N_p}{N_m} \right) \left(\frac{\mu_m}{\mu_p} \right) \left(\frac{D_{sp}}{D_{sm}} \right)^2 = 1 \quad (\text{F14})$$

so that

$$\frac{N_m}{N_p} = \left(\frac{\rho_p}{\rho_m} \right) \left(\frac{\mu_m}{\mu_p} \right) \left(\frac{D_{sp}}{D_{sm}} \right)^2 \quad (F15)$$

If one considers water at 1 atm, 300K (~540R) as a referee fluid, and cryogenic liquid hydrogen saturated at 24.7K (45R) as the prototype fluid, then

$$\left(\frac{\rho_m}{\rho_p} \right) = 15.6 \quad (F16)$$

$$\left(\frac{\mu_m}{\mu_p} \right) = 91 \quad (F17)$$

Substituting these values in the above expressions results in

$$\frac{N_m}{N_p} = \left(\frac{1}{15.6} \right) (91) (30)^2 = 5250 \quad (F18)$$

which is much larger than the assumed ratio of 14. This means that a different referee fluid under the proper thermodynamic state must be sought.

Considering now the Weber number, again,

$$\frac{(N_{we})_p}{(N_{we})_m} = \left(\frac{\rho_p}{\rho_m} \right) \left(\frac{N_p}{N_m} \right)^2 \left(\frac{D_{sp}}{D_{sm}} \right)^3 \left(\frac{\sigma_m}{\sigma_p} \right) = 1 \quad (F19)$$

so that,

$$\frac{N_m}{N_p} = \left(\frac{\rho_p}{\rho_m} \right) \left(\frac{D_{sp}}{D_{sm}} \right)^3 \left(\frac{\sigma_m}{\sigma_p} \right) \quad (F20)$$

For the water-hydrogen combination considered previously,

$$\frac{\sigma_m}{\sigma_p} = 59 \quad (F21)$$

and, in this case,

$$\begin{aligned} \frac{N_m}{N_p} &= \left(\frac{1}{15.6} \right) (30)^3 (59) \\ &= 320 \end{aligned} \quad (F22)$$

which is larger than the assumed value of 14, pointing again to the need for a proper referee fluid.

The power number is useful in predicting power requirements for the prototype once the experimental values for the model are obtained.

Thus,

$$\frac{(N_{p1})_p}{(N_{p1})_m} = \left(\frac{P^1_p}{P^1_m} \right) \left(\frac{\rho_m}{\rho_p} \right) \left(\frac{N_m}{N_p} \right)^3 \left(\frac{D_{sm}}{D_{sp}} \right)^5 = 1 \quad (F23)$$

from which

$$\frac{P^1_p}{P^1_m} = \left(\frac{\rho_p}{\rho_m} \right) \left(\frac{N_p}{N_m} \right)^3 \left(\frac{D_{sp}}{D_{sm}} \right)^5 \quad (F24)$$

The ratio of J_p/J_m is useful in determining proper ratios of flow rates for the liquid discharge since \dot{m}_{efflux} is proportional to V .

CONCLUSION

An initial attempt to provide a model for engineering analysis of a screw settling device used as a means of settling the liquid-vapor phases of a fluid within a tank for subsequent transfer to another vessel, has been presented in this work. Actual tests will indicate the suitability of the model, or provide the basis for necessary modifications.

Similarity analysis indicated that:

- a) it is impractical to carry out tests at one g.
- b) an adequate referee fluid should be sought for tests with a scaled down model of the system.

REFERENCES

1. Holland, F. A., Chapman, F. S., "Liquid Mixing & Processing in Stirred Tanks", Reinhold Publishing Corp., 1966.
2. Spalding, D. B., Cole, E. H., "Engineering Thermodynamics", McGraw Hill Book Co., 1958.
3. Stark, J. A., "Low-G Fluid Transfer Technology", NASA CR-134911/CADS-NAS-76-014, May 1976.
4. Stark, J. A., "Study of Low Gravity Propellant Transfer", Final Report No. GDCA-DDB-72-002/NAS 8-26236, General Dynamics, 1972.
5. Vhl, V. W., Gray, J. B., "Mixing Theory and Practice", Vol. 1., Academic Press, 1966.
6. Wallis, R. A., "Axial Flow Fan Design & Practice", Academic Press, 1961.
7. White, F. M., "Fluid Mechanics", McGraw Hill Book Co., 1979.
8. "Orbital Refueling and Checkout Study, Vol. III - Evaluation of Fluid Transfer Modes", T1-51-67-21 Lockheed Missiles & Space Co., February 1968.